Density and quasiparticle excitations in liquid ^{4}He

H. R. Glyde*
Department of Physics, University of Alberta, Edmonton, Alberta, Canada T6G 2J1
(Received 29 April 1991; revised manuscript received 29 October 1991)

The recent interpretation of the phonon-roton excitations in superfluid ^{4}He as a density mode at low wave vector and a quasiparticle excitation at higher Q proposed by Glyde and Griffin is developed. When there is a condensate, $n_0(T)$, the quasiparticle response of liquid ^{4}He, becomes a component of the observed density dynamic structure factor, $S(Q,\omega)$. The quasiparticle and density response functions also share a common denominator, due to a coupling via the condensate. At low Q, the observed $S(Q,\omega)$ is confined predominantly to a single peak. The peak broadens with temperature but remains well defined in normal ^{4}He, where $n_0(T)=0$. This peak is interpreted as a density mode. At the maxon and higher Q, $S(Q,\omega)$ has a sharp peak plus a broad component. The sharp peak is interpreted as the quasiparticle component of $S(Q,\omega)$. As T is increased and $n_0(T)$ is decreased, the intensity in the sharp peak is reduced until it vanishes from $S(Q,\omega)$ at T_λ. A simple model based on uncoupled quasiparticle and density excitations with coupling via $n_0(T)$ is proposed. For simplicity, all model parameters are held independent of T. By allowing only $n_0(T)$ to vary with T, the temperature dependence of $S(Q,\omega)$ can be quite accurately reproduced.

I. INTRODUCTION

In 1941 Landau[1] proposed two collective excitations in liquid ^{4}He which he called phonons and rotons. The phonons were collective density (sound) modes having dispersion linear in the wave vector, Q. The rotons were a collective rotation of the fluid having a separate dispersion curve. In 1947, Landau[2] joined the phonons and rotons into a single collective mode dispersion curve continuous in Q. Rotons and phonons were then interpreted as the low- and high-Q regions of the same collective excitation. This improved agreement with experiment and was consistent with the continuous dispersion curve for excitations in a dilute Bose gas derived microscopically by Bogoliubov.[3] In this sense the present use of the name "roton" is a misnomer. The phonon-roton dispersion curve is shown in Fig. 1.

Feynman[4] and Feynman and Cohen[5] proposed a microscopic explanation of the excitations introduced phenomenologically by Landau. The excitations were collective density excitations at all Q. The excited state was obtained by operating on the ground state with the density operator,

$$\rho(Q)=\sum_i e^{-iQ\cdot r_i}=\sum_k a_k^\dagger a_{k+Q} \ .$$

While this described the low-Q, phonon region well, at higher Q in the roton region the calculated excitation energy lay significantly above the observed value. The roton energy can be well reproduced by modifying the excitation operator to include backflow and/or interaction with two- or three-density excitation states. Thus, while the density excitation picture works well at low Q, a more complicated state is needed at higher Q. More recent developments of the method are reviewed and presented by Campbell,[6] Chester,[7] and Manousakis and Pandharipande.[7]

The phonon-roton dispersion curve has been accurately measured as a function of Q by inelastic neutron scattering. The phonon-roton energy, which we denote as $\omega(Q)$, is defined as the position of the sharp peak in the inelastic-neutron-scattering intensity. In addition to the sharp peak, there is a broad component[8] in the scattering intensity at higher Q. Early experiments which focused chiefly on low temperature are thoroughly reviewed by Woods and Cowley.[9]

A parallel microscopic theory of Bose fluids based on many-body theory was developed by Beliaev,[10] Hugenholtz and Pines,[11] Gavoret and Nozières,[12] and many others.[13–15] In this theory both density excitations, described by the dynamic susceptibility χ, and

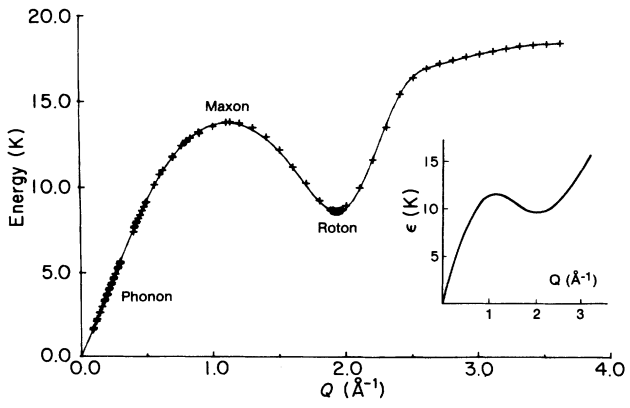

FIG. 1. The phonon-roton dispersion curve in superfluid ^{4}He at SVP and low T with the inset showing the curve proposed by Landau in 1947 (Ref. 2) (from Refs. 24 and 40).

quasiparticle propagation, described by the single-particle Green function G, are studied. In the dilute-Bose-gas limit, Hugenholtz and Pines[11] showed that χ and G are the same function confirming very directly Bogoliubov's results. For a strongly interacting fluid, Gavoret and Nozières[12] showed that the density excitation of χ and the quasiparticle excitations of G have the same linear dispersion curve, $\omega(Q)=c_0Q$, at low Q and $T=0$ K. The finite-temperature formulation of this theory, particularly by Griffin and Cheung[16] and Szépfalusy and Kondor,[17] which emphasizes the coupling between the density and quasiparticle excitations via the condensate and the distinction between normal and superfluid ^{4}He, is the basis of the present model. This theory is generally denoted the dielectric formulation of Bose fluids.

In 1990, Stirling and Glyde[18,19] and Glyde and Griffin[20] proposed another interpretation of the phonon-roton excitations observed in $S(Q,\omega)$. In superfluid ^{4}He where there is a finite fraction, $n_0(T)$, of atoms in the condensate, the total dynamic susceptibility, χ, has two components; the single-particle Green function G with weight in χ depending on $n_0(T)$ and the dynamic susceptibility, χ', of the atoms lying above the condensate. The total χ and G are also coupled via the condensate.[16,17] At low Q the fluid supports a sharply defined collective mode which dominates $S(Q,\omega)$. It is the zero-sound mode characteristic of a strongly interacting fluid proposed by Pines.[21] The mode exists in both superfluid and normal ^{4}He. As Q increases, the mode broadens.[18–20] At the maxon Q ($Q\simeq 1.1$ Å^{-1}), the zero-sound mode is broad. At the roton Q, the observed scattering intensity in normal ^{4}He is very broad, characteristic of an excitation among weakly interacting atoms. The quasiparticle excitation in superfluid ^{4}He is sharply defined at all Q. In this interpretation,[18–20] the sharp peak in $S(Q,\omega)$ at the maxon, roton, and higher Q in superfluid ^{4}He originates from the quasiparticle excitation and disappears from $S(Q,\omega)$ in normal ^{4}He where $n_0(T)=0$. The quasiparticle may be pictured as a renormalized atom that propagates readily in the fluid, much as a ^{3}He impurity can propagate freely in superfluid ^{4}He.

The purpose here is to develop the model of $S(Q,\omega)$ proposed by Glyde and Griffin[20] based on the dielectric-function formulation. The aim is to verify the density-quasiparticle interpretation of excitations in superfluid ^{4}He by reproducing the temperature dependence of $S(Q,\omega)$ in superfluid and normal ^{4}He. The model contains initially uncoupled density and quasiparticle excitations. For simplicity, we assume that the frequency and half-width of each excitation is independent of temperature. This assumption is made to keep the model as simple as possible and to illustrate the fundamental dependence of $S(Q,\omega)$ on $n_0(T)$. The temperature dependence of $S(Q,\omega)$ is obtained by allowing the coupling via the condensate to have a temperature dependence given by $n_0(T)$. Certainly, we expect the half-widths of each excitation to depend upon T and the present model is intended to be illustrative only. Based on the dielectric-function formulation[16,17] we propose that the uncoupled density excitations are broad in both superfluid and normal ^{4}He at $Q\gtrsim 1.1$ Å^{-1} and that a continuous phonon-quasiparticle (phonon-roton) curve results through coupling via the condensate. Since our interpretation is motivated by experiment, we outline some recent results.

In 1978, Woods and Svensson[22] reported key measurements of the temperature dependence of the neutron-scattering intensity at wave vectors ranging from the maxon to the roton region. At low T these showed a sharp peak plus a broad component consistent with earlier data.[9] As T increased, the sharp peak in $S(Q,\omega)$, identified with the phonon-roton excitation at low T, lost intensity until it disappeared from $S(Q,\omega)$ entirely at $T=T_\lambda$. In normal ^{4}He, only broad scattering having no sharp peak remained. These important measurements suggested that the long-lived excitation observed in superfluid ^{4}He disappeared from $S(Q,\omega)$ at $T=T_\lambda$. Understanding these results proved difficult.[23,24]

Talbot *et al.*[25] measured the temperature dependence of $S(Q,\omega)$ at the maxon and roton Q in ^{4}He at 20-bars pressure. These confirmed the basic finding of Woods and Svensson;[22] that the sharp peak of $S(Q,\omega)$ disappeared from $S(Q\omega)$ at $T=T_\lambda$ leaving only board scattering in normal ^{4}He. The data are clearer at 20 bars because the position of the sharp peak and of the maximum in the broad scattering remaining in normal ^{4}He are separated in energy, making it difficult to interpret the results as a simple broadening of the sharp peak with T. The data of Talbot *et al.*[25] at the maxon are reproduced below in Fig. 5.

In order to establish whether the temperature dependence of $S(Q,\omega)$ was the same at all Q, Stirling and Glyde[18] made measurements in the phonon ($Q=0.4$ Å^{-1}) and the roton regions ($Q=1.925$ Å^{-1}) at saturated vapor pressure (SVP). These showed that the temperature dependence was different at low Q. At $Q=0.4$ Å^{-1}, the intensity is confined largely to a single peak. This peak broadens with increasing T, but a well-defined single peak remains in normal ^{4}He above T_λ. As shown earlier by Woods,[26] the peak position changes little with temperature even above T_λ. In the interpretation of Stirling and Glyde[18,19] and Glyde and Griffin[20] the high- and low-Q regions are quite different. At low Q, the sharp peak in $S(Q,\omega)$ represents scattering chiefly from the collective zero-sound mode in the fluid density proposed by Pines,[21,27] Feynman,[4] and Landau[2] which survives in normal ^{4}He. At the maxon and roton Q, the sharp peak in $S(Q,\omega)$ is interpreted as a peak of the single-particle Green function, a quasiparticle excitation. G is coupled into $S(Q,\omega)$ via the condensate in superfluid ^{4}He with weight proportional to $n_0(T)$. As T increases, this coupling weakens and at $T=T_\lambda$ where $n_0(T)=0$, the quasiparticle peak disappears from $S(Q,\omega)$. The coupling via the condensate leads to a continuous density-quasiparticle excitation dispersion curve.

In Sec. II, we outline the dielectric formulation showing that G appears as a component of $S(Q,\omega)$, that χ and G are coupled via the condensate and develop the model of $S(Q,\omega)$. The calculations reproducing the observed structure of $S(Q,\omega)$ at low T and its temperature dependence in superfluid ^{4}He are presented in Sec. III. The results are discussed and calculations of the corresponding quasiparticle spectral function are presented in Sec. IV.

II. DENSITY, QUASIPARTICLE MODEL OF $S(Q,\omega)$

In this section we sketch the dielectric-function formulation of Bose fluids and develop an explicit model of $S(Q,\omega)$ based on it. We begin by showing that, in superfluid ^{4}He, where there is a finite condensate (a Bose broken symmetry), the single-particle Green function describing quasiparticle excitations is a component of the dynamic susceptibility χ. We then illustrate that χ and G are coupled via the condensate. In the last part of this section we propose a model to obtain explicit expressions for the components of χ for comparison with experiment.

The separation of χ into a part containing G and a part χ' describing the atoms above the condensate was first made by Hugenholtz and Pines.[11] The formal separation for a strongly interacting fluid in the form we use was first made by Gavoret and Nozières.[12] We follow closely the development by Griffin and Cheung and by Szépfalusy and Kondor valid at arbitrary temperature. A key feature is the explicit recognition that there is a finite fraction, $n_0=N_0/N$, of the atoms in the zero-momentum state. This means that the number operator $\hat{N}_0$ gives

$$\hat{N}_0|0\rangle=a_0^\dagger a_0|0\rangle=N_0|0\rangle \ , \tag{1}$$

where $N_0\sim 10^{22}\gg 1$. Since $N_0\gg 1$, we may ignore the unity in the commutation relation, $a_0a_0^\dagger-a_0^\dagger a_0=1$, compared with N_0, and replace the single-particle operator a_0 by a number[3,11]

$$a_0=a_0^\dagger=\sqrt{N_0}e^{i\phi} \ . \tag{2}$$

The replacement (2) constitutes the Bose broken symmetry and in a homogeneous fluid we may take $\phi=0$. We now show that, when (2) is used, G is a component of χ with a weight proportional to $n_0(T)$.

A. Density and single-particle excitations

The total density dynamic susceptibility is[16,17,28]

$$\chi(Q,\tau)=-\frac{1}{N}\langle \mathcal{T}_\tau\rho(Q,\tau)\rho^\dagger(Q,0)\rangle \ , \tag{3}$$

which is related to the observed dynamic structure factor by[28,29]

$$S(Q,\omega)=-\frac{1}{\pi}[n(\omega)+1]\chi''(Q,\omega) \ , \tag{4}$$

where $n(\omega)$ is the Bose function. In second quantization, the Fourier component of the density operator is

$$\rho(Q)=\sum_k a_k^\dagger a_{k+Q} \ , \tag{5}$$

where $a_k^\dagger$ is the single-particle operator creating a quasiparticle having momentum k. In Bose condensation theory it is necessary to separate the atoms in the condensate from those N' lying above the condensate, $N=N_0+N'$. We make the same separation for $\rho(Q)$,

$$\begin{aligned}\rho(Q)&=a_0^\dagger a_Q+a_{-Q}^\dagger a_0+\sum_k{}' a_k^\dagger a_{k+Q}\\ &\equiv\sqrt{N_0}\,A_Q+\rho'(Q) \ ,\end{aligned} \tag{6}$$

where terms involving $k=0$ are written separately and the primed sum involves atoms above the condensate only. In the second line of (6) we have used (2). $A_Q=(a_Q+a_{-Q}^\dagger)$ is a sum of single-particle operators and $\rho'(Q)$ is the usual density operator describing atoms above the condensate. Substitution of (6) into (3) leads to

$$\begin{aligned}\chi(Q,\tau)=n_0G(Q,\tau)&-\frac{\sqrt{N_0}}{N}\langle \mathcal{T}_\tau A_Q(\tau)\rho^{\dagger\prime}(Q,0)+\text{H.c.}\rangle\\ &+\chi'(Q,\tau) \ .\end{aligned} \tag{7}$$

The first term, proportional to n_0, is the single-particle Green function

$$G(Q,\tau)=-\langle \mathcal{T}_\tau A_Q(\tau)A_Q^\dagger(0)\rangle \ ,$$

the second term is an interference term between the single particle and density excitations, and the last term

$$\chi'(Q,\tau)=-N^{-1}\langle \mathcal{T}_\tau\rho'(Q,\tau)\rho^{\dagger\prime}(Q,0)\rangle$$

is the usual density dynamic susceptibility involving atoms above the condensate.

When there is a condensate, the Hamiltonian contains terms of the form[11] $(\sqrt{N_0}/V)\sum'_{q,k}v(q)a_q^\dagger a_k^\dagger a_{k+q}$ having three single-particle operators. Because of these terms, the interference terms do not vanish and are also proportional to the single-particle G. The Fourier transform of $\chi(Q,\tau)$ is[12]

$$\chi(Q,\omega)=\Lambda(Q,\omega)G(Q,\omega)\Lambda(Q,\omega)+\chi'(Q,\omega) \ , \tag{8}$$

where the vertex function $\Lambda(Q,\omega)$ takes the form

$$\Lambda(Q,\omega)=(n_0)^{1/2}[1+P(Q,\omega)] \ .$$

In Λ the unit term arises from the first term of (7) and $P(Q,\omega)$ is a complicated function arising from the interference terms. Parenthetically we note that the density dynamic susceptibility in an anharmonic solid may also be expressed[30] in the form (8), as discussed further in Sec. IV. In an anharmonic solid, G is the e single-phonon Green function. There, the interference terms arise because of the odd anharmonic terms in H, notably the cubic anharmonic term.

In superfluid ^{4}He, the quasiparticle excitations of G are coupled into χ via the vertex functions Λ which are proportional to $n_0(T)$. We interpret the sharp peak in $S(Q,\omega)$ at the maxon and roton regions as a sharp peak in G, a quasiparticle excitation. While (8) is illustrative, we now go on to show that the density excitations described by χ and the quasiparticle excitations described by G are strongly coupled via the condensate in superfluid ^{4}He. A model description of this coupling is proposed to describe the temperature dependence of $S(Q,\omega)$.

B. Dielectric formulation

In the dielectric formulation of Bose liquids we write the dynamic susceptibility as[16,17]

$$\begin{aligned}\chi&=\tilde{\chi}+\tilde{\chi}v(Q)\tilde{\chi}+\tilde{\chi}v(Q)\tilde{\chi}v(Q)\tilde{\chi}+\cdots\\ &=\frac{\tilde{\chi}}{1-v(Q)\tilde{\chi}}=\frac{\tilde{\chi}}{\epsilon} \ .\end{aligned} \tag{9}$$

Here $\tilde{\chi}$ is the irreducible χ, that part of $\tilde{\chi}$ which cannot be reduced to two parts separated by a single interaction line, $v(Q)$. Equation (9) may be regarded as the definition of $\tilde{\chi}$. Equation (9) can be derived diagrammatically using that part of the Hamiltonian having four single-particle operators describing the atoms above the condensate only. In (9), ϵ is the dielectric function

$$\epsilon \equiv 1 - v(Q)\tilde{\chi} \ . \tag{10}$$

As in (8), the irreducible $\tilde{\chi}$ may be decomposed into a singular and regular part,[17]

$$\tilde{\chi} = \tilde{\chi}_S + \tilde{\chi}_R = \tilde{\Lambda}\tilde{G}\tilde{\Lambda} + \tilde{\chi}_R \ , \tag{11}$$

where $\tilde{\Lambda} = (n_0)^{1/2}[1+\tilde{P}(Q,\omega)]$ is the vertex function which vanishes in normal ^{4}He. Clearly, in normal ^{4}He the full dielectric function (10) reduces to its regular counterpart,

$$\epsilon_R \equiv 1 - v(Q)\tilde{\chi}_R \ . \tag{12}$$

In superfluid ^{4}He, $\epsilon = \epsilon_R - v(Q)\tilde{\Lambda}\tilde{G}\tilde{\Lambda}$.

The $\tilde{G}$ introduced in (11) may be denote the "regular" or "uncoupled" G. It is the single-particle G taking account of the interaction between the quasiparticles above the condensate but neglecting the terms involving the condensate. Generally, the full G is given by

$$G^{-1} = G_0^{-1} - \Sigma \ , \tag{13}$$

where G_0 is the single-particle Green function for a noninteracting Bose gas and Σ is the total self energy. We separate Σ into two parts, $\Sigma = \tilde{\Sigma} + M$, where $\tilde{\Sigma}$ arises from terms in H describing the atoms above the condensate only and M from terms in H involving the condensate. Formally, we have[17]

$$\begin{aligned} G^{-1} &= G_0^{-1} - \tilde{\Sigma} - M \\ &= \tilde{G}^{-1} - M \ , \end{aligned} \tag{14}$$

where $\tilde{G}^{-1} \equiv G_0^{-1} - \tilde{\Sigma}$. It can be shown[17] that $M = \tilde{\Lambda} v(Q) \tilde{\Lambda}/\epsilon_R$.

Collecting results, we have in superfluid ^{4}He, for $T < T_\lambda$,

$$\begin{aligned} &\chi = \tilde{\chi}/\epsilon \ , \quad \tilde{\chi} = \tilde{\Lambda}\tilde{G}\tilde{\Lambda} + \tilde{\chi}_R \ , \\ &G = \frac{N}{D} \ , \quad G^{-1} = \tilde{G}^{-1} - M \ , \end{aligned} \tag{15}$$

and in normal ^{4}He, where $\tilde{\Lambda} = 0$,

$$\begin{aligned} &\chi = \tilde{\chi}_R/\epsilon_R, \quad \tilde{\chi}_R = \tilde{N}_R/\tilde{D}_R \ , \\ &\tilde{G} = \frac{\tilde{N}}{\tilde{D}} \ , \quad \tilde{G} = G_0^{-1} - \tilde{\Sigma} \ . \end{aligned} \tag{16}$$

In normal ^{4}He, where $M = 0$, $\tilde{G}$ is the total Green function. The $\tilde{G}$ becomes coupled into χ via the vertex function $\tilde{\Lambda} = (n_0)^{1/2}[1+\tilde{P}(Q,\omega)]$ in superfluid ^{4}He. Similarly, the density dielectric function ϵ_R is coupled into the single-quasiparticle Green function G in the superfluid phase, via $\tilde{\Lambda}$ and M. In normal ^{4}He, where $\tilde{\Lambda} = 0$, χ and G are independent.

We now display more fully how χ and G are coupled and that χ and G share a common denominator in the superfluid phase where $\tilde{\Lambda} \neq 0$. The present formulation is somewhat different from the usual one.[16,17] The present expressions lead naturally into the model proposed below.

Below T_λ we have, from (10), (11), and (16),

$$\begin{aligned} \epsilon &= 1 - v(Q)\tilde{\Lambda}\tilde{G}\tilde{\Lambda} - v(Q)\tilde{\chi}_R \\ &= 1 - \frac{\Delta}{\tilde{D}} - \frac{\alpha}{\tilde{D}_R} \ , \end{aligned} \tag{17}$$

where $\Delta \equiv v(Q)\tilde{\Lambda}\tilde{N}\tilde{\Lambda}$ is the coupling parameter and $\alpha \equiv v(Q)\tilde{N}_R$. Rearranging, we have

$$\frac{1}{\epsilon} = \frac{\tilde{D}\tilde{D}_R}{\tilde{D}\tilde{D}_R - \Delta\tilde{D}_R - \alpha\tilde{D}} \equiv \frac{\tilde{D}\tilde{D}_R}{R + i\Gamma} \ . \tag{18}$$

From (9) and (10), we have

$$\chi = \frac{\tilde{\chi}}{\epsilon} = \frac{1}{v(Q)}\frac{1-\epsilon}{\epsilon} = \frac{1}{v(Q)}\left[\frac{1}{\epsilon} - 1\right] \ , \tag{19}$$

and using (18), we have

$$\chi = \frac{1}{v(Q)}\left[\frac{\tilde{D}\tilde{D}_R(R - i\Gamma)}{R^2 + \Gamma^2} - 1\right] \ . \tag{20}$$

Similarly,

$$\begin{aligned} G^{-1} &= \tilde{G}^{-1} - M = \tilde{G}^{-1}[1 - \tilde{G}\tilde{\Lambda}v(Q)\tilde{\Lambda}/\epsilon_R] \\ &= \tilde{G}^{-1}[\epsilon_R - v(Q)\tilde{\Lambda}\tilde{G}\tilde{\Lambda}]/\epsilon_R = \tilde{G}^{-1}\epsilon/\epsilon_R \ . \end{aligned} \tag{21}$$

Writing $\epsilon_R = 1 - v(Q)\tilde{N}_R/\tilde{D}_R$ and using (16)–(18), we obtain

$$G = \frac{\tilde{N}(\tilde{D}_R - \alpha)}{R + i\Gamma} = \frac{\tilde{N}(\tilde{D}_R - \alpha)(R - i\Gamma)}{R^2 + \Gamma^2} \ . \tag{22}$$

In this way we see, comparing (20) and (22), that the density (χ'') and quasiparticle (G'') spectral functions share a common denominator, $R^2 + \Gamma^2$. In normal ^{4}He, where $\tilde{\Lambda}$ and Δ vanish, we can readily see that χ_R and G decouple and become independent.

C. The model

To implement the dielectric formulation for liquid ^{4}He, we propose a specific model for the "regular" dynamic susceptibility $\tilde{\chi}_R = \tilde{N}_R/\tilde{D}_R$, and the "regular" Green function, $\tilde{G} = \tilde{N}/\tilde{D}$, defined in (11) and (14), respectively. These are the dynamic susceptibility $\tilde{\chi}_R$ and single-particle Green function $\tilde{G}$ obtained by taking account of the interaction between the atoms lying above the condensate. They may also be called the "uncoupled" functions. $\tilde{\chi}_R$, and $\tilde{G}$ become the full functions in normal ^{4}He, where $n_0 = 0$. Since n_0 is not large, then $\tilde{\chi}_R$ and $\tilde{G}$ might be approximately independent of temperature. However, since there is a significant redistribution of atoms among the finite momentum states between low T and normal ^{4}He, we do expect some temperature dependence of $\tilde{\chi}_R$ and $\tilde{G}$.

The dynamic susceptibility may be separated into a sin-

gle quasiparticle-hole and a multiquasiparticle-hole component,[8,32] which we write here as

$$\tilde{\chi}_R = \tilde{\chi}_0 + \tilde{\chi}_M \ . \tag{23}$$

We neglect the multiquasiparticle-hole part, $\tilde{\chi}_M$, here. This means we will leave out the interesting effects which lead to subsidiary peaks in $S(Q,\omega)$ above the main peak, generally attributed to excitation of pairs of rotons or other pairs.[7,31] We may expect the intensity in the present model to be too small at higher ω where $\tilde{\chi}_M$ contributes most. Neglecting $\tilde{\chi}_M$, we present $\tilde{\chi}_R$ as

$$\tilde{\chi}_R = \frac{\tilde{N}_R}{\tilde{D}_R} \approx \tilde{\chi}_0 = \frac{\tilde{N}_R}{\omega^2 - \Omega^2 + i2\omega\Gamma_0} \ . \tag{24}$$

Equation (24) may be regarded as an approximation to the interacting particle-hole susceptibility (i.e., a modified Lindhard function in Fermi systems) where Ω and Γ_0 are parameters describing the energy and half-width of the quasiparticles. $\tilde{N}_R(Q)$ is a function which at low Q (where $\tilde{\chi}_M \to 0$) must be proportional to Q^2 to satisfy the f-sum rule.

For the uncoupled $\tilde{G}$ we choose the general Bose particle form

$$\tilde{G} = \frac{\tilde{N}}{\tilde{D}} = \frac{2\bar{\omega}_{SP}}{\omega^2 - \bar{\omega}_{SP}^2 + i2\omega\Gamma_{SP}} \ . \tag{25}$$

This may be obtained from (16), $\tilde{G} = G_0^{-1} - \Sigma$, using G_0 for free Bosons, $G_0 = 2\omega_{SP}^2/(\omega^2 - \omega_{SP}^{0\,2})$, and parametrizing the self-energy as $\Sigma = \Sigma' - i\Gamma_{SP}$, where $\bar{\omega}_{SP}^2 \equiv \omega_{SP}^{02} + 2\omega_{SP}^0\Sigma'$. We have also assumed $\omega_{SP}^0\Gamma_{SP} \approx \omega\Gamma_{SP}$ and taken $\omega_{SP}^0 \approx \bar{\omega}_{SP}$ in the numerator of $\tilde{G}$. Equation (25) is often used to describe single Bosons such as phonons. Equations (24) and (25) may be regarded as model for two uncoupled Bose excitations, one in the density and one for a single particle.

1. *Dynamic structure factor*

In normal ^{4}He we have, using (24),

$$\chi = \frac{\tilde{\chi}_R}{\epsilon_R} = \frac{\chi_0}{1 - v(Q)\chi_0} = \frac{\tilde{N}_R}{\tilde{D}_R - \alpha} = \frac{\tilde{N}_R}{\omega^2 - \bar{\omega}_0^2 + i2\omega\Gamma_0} \ , \tag{26}$$

where $\bar{\omega}_0^2 \equiv \Omega^2 + \alpha$ and $\tilde{N}_R = F(Q)2\Omega$. The dynamic structure factor is ($T > T_\lambda$)

$$S(Q,\omega) = -\frac{1}{\pi}[n(\omega)+1]\chi''(Q,\omega) = \frac{\tilde{N}_R}{\pi}[n(\omega)+1]\frac{2\omega\Gamma_0}{(\omega^2 - \bar{\omega}_0^2)^2 + (2\omega\Gamma_0)^2} \ . \tag{27}$$

Equation (27) is often called[25,33] the "harmonic-oscillator" function. It is used as a function to fit to observed data and $\bar{\omega}_0$ and Γ_0 are identified as the excitation energy and half-width, respectively. In normal ^{4}He, $S(Q,\omega)$ describes density excitations only. At low Q, where we expect normal ^{4}He to support a zero-sound mode, $\bar{\omega}_0$ and Γ_0 may be clearly interpreted as the uncoupled zero-sound mode energy and half-width (inverse lifetime), respectively, with $\Gamma_0 \ll \bar{\omega}_0$. At higher Q (e.g., maxon and roton Q's), where we expect a broad or no zero-sound mode, ω_0 may be interpreted as a characteristic energy describing weakly interacting quasiparticle-hole excitations. We use this interpretation here and fit (27) to observed data to determine $\bar{\omega}_0$ and Γ_0.

In superfluid ^{4}He, the imaginary part of χ is

$$\chi'' = \frac{1}{v(Q)}\left[\frac{1}{\epsilon}\right]'' = \frac{1}{v(Q)}\left[\frac{\tilde{D}\tilde{D}_R}{R + i\Gamma}\right] \ . \tag{28}$$

Defining $\gamma_{SP} = 2\omega\Gamma_{SP}$ and $\gamma_0 = 2\omega\Gamma_0$, (24) and (25) give

$$\tilde{D}\tilde{D}_R = (\omega^2 - \Omega^2 + i\gamma_0)(\omega^2 - \bar{\omega}_{SP}^2 + i\gamma_{SP}) \tag{29}$$

and

$$\begin{aligned} R + i\Gamma &= \tilde{D}\tilde{D}_R - \Delta\tilde{D}_R - \alpha\tilde{D} \\ &= (\tilde{D} - \Delta)(\tilde{D}_R - \alpha) - \Delta\alpha \\ &= [(\omega^2 - \bar{\omega}_0^2)(\omega^2 - \tilde{\omega}_{SP}^2) - \Delta\alpha - \gamma_{SP}\gamma_0] \\ &\quad + i[\gamma_0(\omega^2 - \tilde{\omega}_{SP}^2) + \gamma_{SP}(\omega^2 - \bar{\omega}_0^2)] \ , \end{aligned} \tag{30}$$

where $\tilde{\omega}_{SP}^2 = \bar{\omega}_{SP}^2 + \Delta$, which leads to

$$S(Q,\omega) = \frac{\tilde{N}_R}{\pi}[n(\omega)+1]\frac{\{\gamma_0(\omega^2 - \bar{\omega}_{SP}^2)^2 + \gamma_{SP}(\Delta/\alpha)(\omega^2 - \Omega^2)^2 + \gamma_{SP}\gamma_0[\gamma_{SP} + (\Delta/\alpha)\gamma_0]\}}{R^2 + \Gamma^2} \ . \tag{31}$$

This rather complicated expression reduces to a transparent, readily interpreted form if we assume the quasiparticle width, Γ_{SP}, is zero ($\gamma_{SP} = 0$),

$$S(Q,\omega) = \frac{\tilde{N}_R}{\pi}[n(\omega)+1]\frac{(2\omega\Gamma_0)(\omega^2 - \bar{\omega}_{SP}^2)^2}{[(\omega^2 - \omega_0^2)(\omega^2 - \omega_{SP}^2)]^2 + [2\omega\Gamma_0(\omega^2 - \tilde{\omega}_{SP}^2)]^2} \ , \tag{32}$$

where

$$R=(\omega^2-\bar{\omega}_0^2)(\omega^2-\tilde{\omega}_{SP}^2)-\Delta\alpha$$
$$\equiv(\omega^2-\omega_0^2)(\omega^2-\omega_{SP}^2) \quad (33)$$

and

$$\tilde{\omega}_{SP}^2=\bar{\omega}_{SP}^2+\Delta\ ,\quad \bar{\omega}_0^2=\Omega^2+\alpha\ . \quad (34)$$

Here $\tilde{\omega}_{SP}$ (or $\bar{\omega}_{SP}$) and $\bar{\omega}_0$ may be interpreted as the "uncoupled" quasiparticle and density frequencies, respectively, in superfluid ^{4}He. In R these become coupled via $\Delta\alpha$ (and $\gamma_{SP}\gamma_0$). ω_{SP} and ω_0 are the shifted frequencies due to the coupling via the condensate. In (32) the width $\Gamma=2\omega\Gamma_0(\omega^2-\tilde{\omega}_{SP}^2)$ vanishes at $\omega=\tilde{\omega}_{SP}$ and we expect $S(Q,\omega)$ to be large near $\tilde{\omega}_{SP}$. Also, the numerator of (32) vanishes at $\omega=\bar{\omega}_{SP}$. Thus, we expect a dip in $S(Q,\omega)$ at $\omega=\bar{\omega}_{SP}$ and the position of this dip in $S(Q,\omega)$ will allow us to determine $\bar{\omega}_{SP}$. When $\Delta=0$, (31) and (32) reduce to (27).

$S(Q,\omega)$ in (32) has five parameters, $\bar{\omega}_0$, Γ_0, $\bar{\omega}_{SP}$, Δ, and α. We determine $\bar{\omega}_0(Q)$ and $\Gamma_0(Q)$, characterizing the uncoupled density response, by fitting $S(Q,\omega)$ in (27) to the observed scattering intensity in normal ^{4}He at each Q. We determine $\bar{\omega}_{SP}(Q)$ by the position of the dip in the observed intensity for $T<T_\lambda$. $\Delta(Q,T)$ and $\alpha(Q)$ are obtained by fitting (32) to the intensity observed at the lowest temperature.

2. *Quasiparticle spectral function*

From (22), (24), and (25), the quasiparticle spectral function is

$$A(Q,\omega)=-2G''(Q,\omega)$$
$$=\frac{4\bar{\omega}_{SP}[\gamma_{SP}(\omega^2-\bar{\omega}_0^2)^2+\gamma_0\Delta\alpha+\gamma_{SP}\gamma_0^2]}{R^2+\Gamma^2}\ , \quad (35)$$

where R and Γ are defined in (30). Comparing (31) and (35) we see that the density and quasiparticle spectral function have the same denominator. Thus, if the spectral functions are sharp, such as at low T and low Q, the density and quasiparticle response of the fluid is the same. In this sense, the density and quasiparticle excitations are one and the same excitation when they are sharp, which we expect to be the case at low Q. Also, so long as $S(Q)$ is independent of T, then, from the f-sum rule, the mode energy of a sharp node will be independent of T. Thus, at low Q in superfluid ^{4}He the density and quasiparticle response is the same and the excitation could be equally called a density or quasiparticle mode.

III. COMPARISON WITH EXPERIMENT

In the previous section, we set out a simple model of $S(Q,\omega)$ in superfluid ^{4}He using the dielectric formulation of Bose fluids. We obtained the specific result (32) by representing the regular or uncoupled density dynamic susceptibility , $\tilde{\chi}_R$, and the single-particle (SP) propagator, $\tilde{G}$, by (24) and (25), respectively. The $\tilde{\chi}_R$ and $\tilde{G}$ are the density and SP propagators taking account of the interaction between the atoms lying above the condensate only. In normal ^{4}He, where $n_0=0$, $\tilde{\chi}_R$ and $\tilde{G}$ are the total χ and G, respectively. In superfluid ^{4}He, the uncoupled quasiparticle excitations described by $\tilde{G}$ are coupled into $S(Q,\omega)$ through the coupling parameters $\Delta=v(Q)2\bar{\omega}_{SP}\tilde{\Lambda}^2$, where

$$\tilde{\Lambda}(Q,\omega)=(n_0)^{1/2}[1+\tilde{P}(Q,\omega)]\ .$$

$\bar{\omega}_{SP}$ and Γ_{SP} are the "uncoupled" quasiparticle frequency and half-width, respectively. In (32) we have taken $\Gamma_{SP}=0$. In normal ^{4}He, where $\Delta(T)=0$, $S(Q,\omega)$ in (32) reduces to (27). As is usual in most fluids, $S(Q,\omega)$ in normal ^{4}He depends only on the uncoupled density response, described here by the frequency $\bar{\omega}_0$ and half-width Γ_0

In this section we compare $S(Q,\omega)$ calculated from (32) and (27) with experiment. The aim is to see whether the basic picture of quasiparticle excitations coupled into $S(Q,\omega)$ via the condensate can reproduce the remarkable temperature dependence of $S(Q,\omega)$ observed in the maxon and roton regions. At each Q we first fit (27) to the observed intensity in normal ^{4}He. This determines $\bar{\omega}_0$ and Γ_0, the uncoupled density excitation parameters. $\bar{\omega}_{SP}$, $\Delta(T)$, and α are determined by fitting $S(Q,\omega)$ in (32) to the lowest-temperature data in superfluid ^{4}He. For simplicity $\bar{\omega}_0$, Γ_0, $\bar{\omega}_{SP}$, and α are assumed to be independent of temperature. The temperature dependence of $S(Q,\omega)$ is obtained using $\Delta(T)\propto n_0(T)$ and assuming $n_0(T)$ follows the Bose gas form so that

$$\Delta(T)=\Delta(0)[1-(T/T_\lambda)^\alpha] \quad (36)$$

with $\alpha=\frac{3}{2}$. $S(Q,\omega)$ is folded with the appropriate instrument resolution to compare with experiment. We begin with the maxon at $p=20$ bars where the sharp peak at low T and density excitation peak in normal ^{4}He are well separated in energy, thus providing a clear example.

A. $p=20$ bar

1. *Maxon*

We begin with normal ^{4}He. In Fig. 2 we compare (27) for normal ^{4}He using $\bar{\omega}_0=0.5$ THz and $\Gamma_0=0.25$ THz with the intensity observed by Talbot *et al.*[25] at $Q=1.13$ Å^{-1} (maxon) and $T=1.90$ K ($T_\lambda=1.928$ K). Near T_λ and above, the observed intensity is largely independent of T. In Fig. 2 the scattering intensity is clearly broad and centered at high energy, $\bar{\omega}_0=0.5$ THz$\simeq$2.0 meV$\simeq$20 K, characteristic of a broadened zero-sound mode. There is additional intensity in the data at higher ω ($\omega>\bar{\omega}_0$) that is not well reproduced in the present model of $S(Q,\omega)$, which we attribute to multiexcitations.

With $\bar{\omega}_0$ and Γ_0 fixed at their T_λ values, we compare $S(Q,\omega)$ for superfluid ^{4}He calculated from (32) with the scattered intensity observed[25] at $T=1.29$ K in Fig. 3. The numerator of (32) has a zero at $\omega=\bar{\omega}_{SP}$. We identify this zero with the dip in the observed intensity just above the sharp quasiparticle peak in Fig. 3. The dip in the intensity observed at 20 bars is not very pronounced. In Fig. 4 we show the intensity observed by Stirling[31] at the

maxon wave vector as a function of pressure. At SVP the observed dip is very pronounced. The uncoupled SP frequency, $\bar{\omega}_{SP}=0.31$ THz, is set in this model by the position of the observed dip in the data.

From Fig. 3, we see that $S(Q,\omega)$ calculated from (32) has a sharp peak at $\omega_{SP}\approx 0.30$ THz. Δ and α in (32) have been adjusted to reproduce the height and position of the peak in the observed scattering intensity. Once $\bar{\omega}_{SP}$ is fixed, the peak height and position are most sensitive to Δ—which determines $\tilde{\omega}_{SP}^2=\bar{\omega}_{SP}^2+\Delta$ and the coupled quasiparticle energy, ω_{SP}, via the R of (3). Since the quasiparticle peak in (32) occurs near $\tilde{\omega}_{SP}$ (or near ω_{SP}), the sign of Δ can be inferred from the position of the quasiparticle peak relative to $\bar{\omega}_{SP}$. This requires $\Delta<0$ for the maxon. $S(Q,\omega)$ is relatively insensitive to α. A 50% change in α changes the quasiparticle peak height little. In Fig. 3, $S(Q,\omega)$ has been folded with the observed instrument resolution width which prevents $S(Q,\omega)$ from going exactly to zero at $\omega=\bar{\omega}_{SP}$. For $\Delta\alpha>0$, the coupled peaks separate, $|\omega_0-\omega_{SP}|>|\bar{\omega}_0-\tilde{\omega}_{SP}|$. We have taken $\Gamma_{SP}=0$. The parameters are listed in Table I.

The temperature dependence of $S(Q,\omega)$ is obtained by holding the parameters in Table I constant except Δ and allowing the coupling parameter $\Delta(T)$ to vary according to the Bose-gas result (36). This is done for simplicity and to display the key dependence of $S(Q,\omega)$ on $n_0(T)$. From Fig. 5 we see this reproduces the observed loss of intensity in the sharp quasiparticle peak with increasing T—until the quasiparticle peak disappears from $S(Q,\omega)$

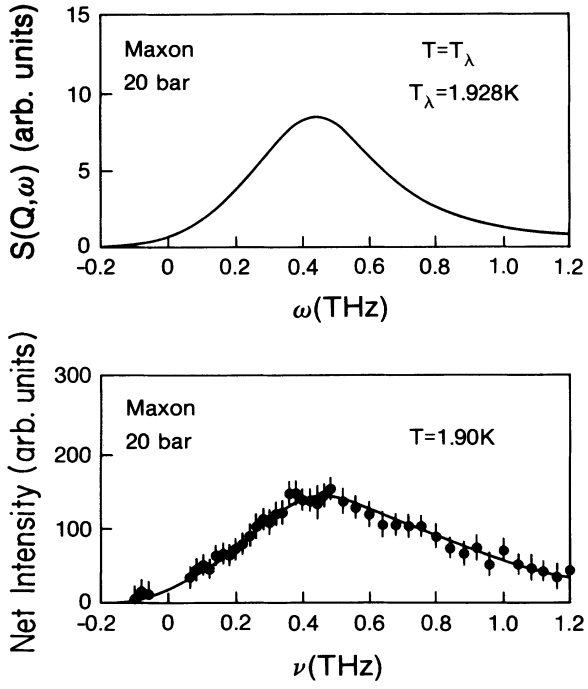

FIG. 2. Maxon, $Q=1.13$ Å^{-1} at $p=20$ bars and $T=T_\lambda$: $S(Q,\omega)$ from (27) with $\bar{\omega}_0=0.50$ THz and $\Gamma_0=0.25$ THz at $T_\lambda=1.928$ K folded with a Gaussian of FWHM of 0.039 THz and the net intensity observed at $T=1.90$ K (Ref. 25).

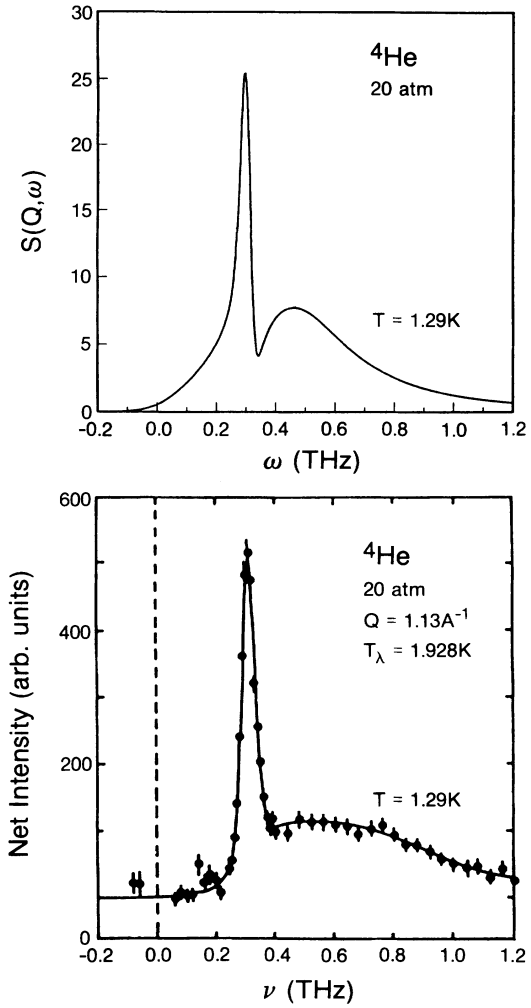

FIG. 3. Maxon, $Q=1.13$ Å^{-1} at $p=20$ bars and $T=1.29$ K: $S(Q,\omega)$ from (32) with $\bar{\omega}_0=0.50$ THz, $\Gamma_0=0.25$ THz, $\bar{\omega}_{SP}=0.31$ THz, $\alpha=-0.5\bar{\omega}_0^2$, and $\Delta=0.005$ THz^2 folded as in Fig. 2 compared with the net intensity observed at $T=1.29$ K (Ref. 25).

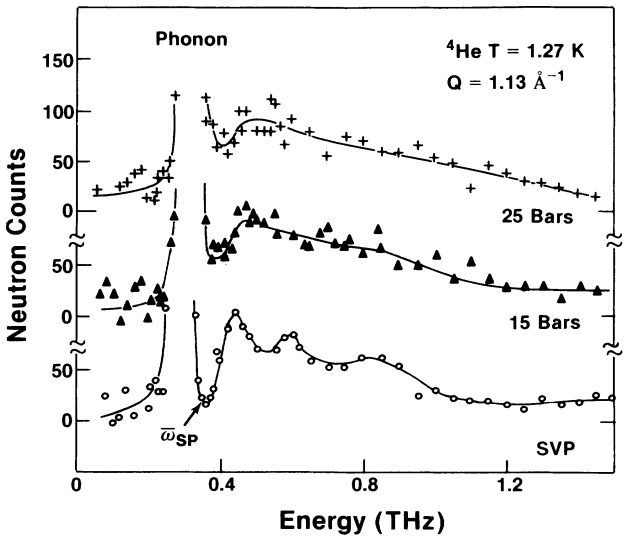

FIG. 4. Maxon, $Q=1.13$ Å^{-1} showing identification of $\bar{\omega}_{SP}$ (data from Ref. 31).

TABLE I. Parameters for $S(Q,\omega)$ in (32) used in Figs. 1–5 for the maxon and in Fig. 6 for the roton at $p=20$ bars. $\bar{\omega}_0$ and Γ_0 are the uncoupled density excitation frequency and half-width (in THz). $\bar{\omega}_{SP}$ and Γ_{SP} are the uncoupled quasiparticle frequency and half-width (in THz). $\Delta=v(Q)\bar{\Lambda}^2 2\bar{\omega}_{SP}$ is the value of the parameter coupling the two excitations via the condensate at the lowest observed temperature (in THz^2) and $\alpha=v(Q)F(Q)2\Omega$. $\omega(Q)$ is the peak position of the resulting sharp peak at the lowest temperature, the phonon-roton energy (in THz).

Q (Å^{-1})	$\bar{\omega}_0$	Γ_0	$\bar{\omega}_{SP}$	Γ_{SP}	Δ	$\alpha/\bar{\omega}_0^2$	$\omega(Q)$
1.13 (maxon)	0.50	0.25	0.31	0	−0.005	−0.5	0.30
2.03 (roton)	0.125	0.075	0.124	0	0.0085	0.4	0.16

entirely at $T=T_\lambda$. This shows that the loss of intensity in the quasiparticle peak can be reproduced by taking $\Delta \propto n_0(T)$ and giving the condensate a plausible temperature dependence. The intensity in the density component changes little with T in Fig. 5. We believe this is because $\bar{\omega}_{SP}$ and $\bar{\omega}_0$ are taken as constant and are well separated from one another for the maxon at $p=20$ bars.

2. Roton

The parameters in $S(Q,\omega)$ for the roton at 20 bars were determined exactly as above for the maxon. The resulting parameters are listed in Table I and $S(Q,\omega)$ for five temperatures is shown in Fig. 6. $S(Q,\omega)$ shows several interesting features. Firstly, $S(Q,\omega)$ at $T=T_\lambda$ is very broad characteristic of scattering from weakly interacting particle-hole pairs rather than from a collective excitation. This leads a large Γ_0, $\Gamma_0 \simeq \bar{\omega}_0$. At low temperature in superfluid ^{4}He, $S(Q,\omega)$ is confined largely to a single sharp peak at the quasiparticle frequency. Thus, although n_0 is small, the coupling via the condensate can confine essentially all the intensity into the quasiparticle peak at low T. Thirdly, the intensity below the sharp quasiparticle peak is significantly reduced as T decreases. Thus, as T decreases, the density component loses intensity. This loss of intensity results when $\bar{\omega}_{SP}$ lies close to $\bar{\omega}_0$ so that the zero in the numerator of $S(Q,\omega)$ at $\omega=\bar{\omega}_{SP}$

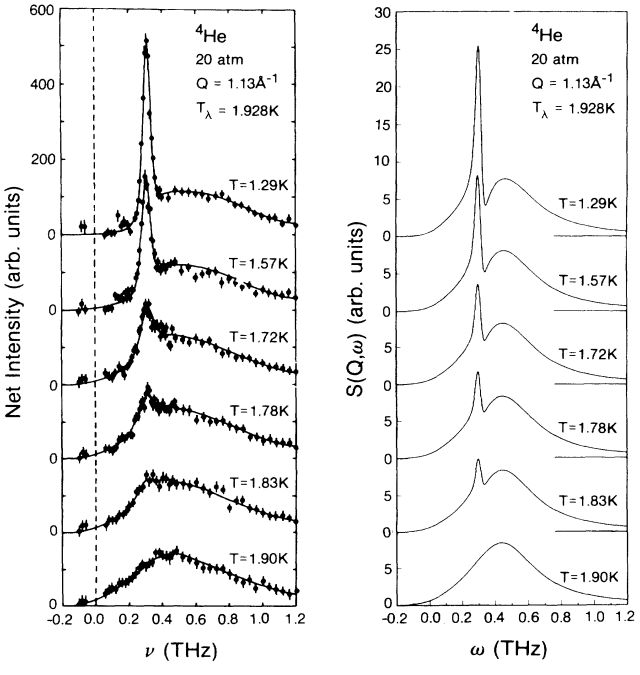

FIG. 5. Maxon, $Q=1.13$ Å^{-1} at $p=20$ bars, temperature dependence: $S(Q,\omega)$ with parameters as in Fig. 3 but $\Delta(T)=\Delta(0)[1-(T/T_\lambda)^{3/2}]$ [$\Delta(0)=0.011$ THz^2] and folded with a Gaussian of FWHM of 0.039 THz compared with net intensity from Ref. 25.

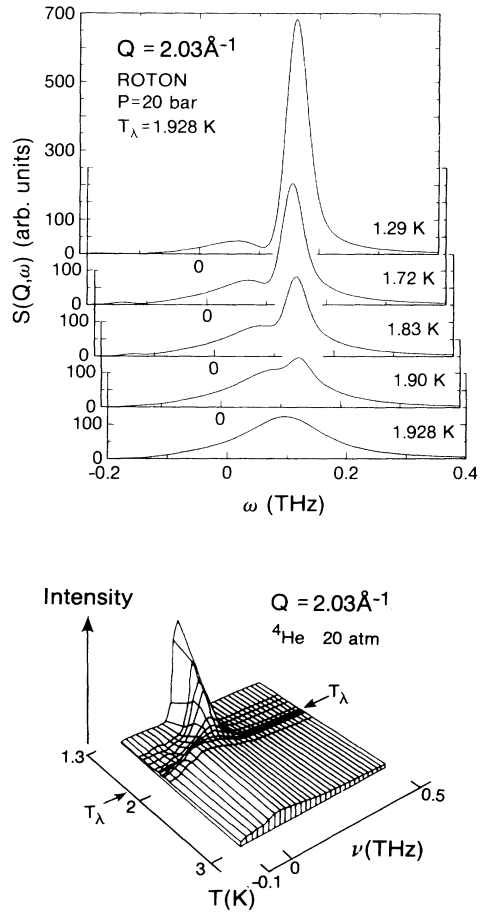

FIG. 6. Roton, $Q=2.03$ Å at $p=20$ bars, temperature dependence: $S(Q,\omega)$ from (32) with parameters listed in Table I and $\Delta(T)=\Delta(0)[1-(T/T_\lambda)^{3/2}]$ folded with a Gaussian of FWHM of 0.036 THz compared with net intensity from Ref. 25.

reduces the intensity in the density component to zero.

The values of the parameters are also interesting. For the roton, the e peak in the density component ($\omega \approx \bar{\omega}_0$) at $T = T_\lambda$ lies below the quasiparticle peak. Thus, we have chosen $\bar{\omega}_0$ marginally less than $\bar{\omega}_{SP}$ so that the coupling can push $\bar{\omega}_{SP}$ upward. Also, at low T, $\bar{\omega}_{SP}$ lies below the quasiparticle peak, $\omega(Q)$. Since the peak position $\omega(Q)$ is determined partly by $\bar{\omega}_{SP}^2 = \bar{\omega}_{SP}^2 + \Delta$, this requires $\Delta > 0$. Also, since the quasiparticle peak position increases with decreasing T, we have $|\omega_{SP} - \omega_0| > |\bar{\omega}_{SP} - \bar{\omega}_0|$. That is, the coupling again separates the quasiparticle and density frequencies requiring $\Delta\alpha > 0$. Thus, both Δ and α change sign from the maxon case. The values of $\bar{\omega}_{SP}(Q)$, $\bar{\omega}_0(Q)$, and the quasiparticle peak, $\omega(Q)$, are sketched in Fig. 7.

B. Saturated vapor pressure

At saturated vapor pressure the position of the quasiparticle peak at low T, $\omega(Q)$, lies close to the position of the maximum of the scattering for $T > T_\lambda$. It is for this reason that it is difficult to decide from the SVP data whether the quasiparticle peak disappears from $S(Q,\omega)$ as T is increased or whether the quasiparticle peak simply broadens with increasing T. In the present model, it means that the "uncoupled" quasiparticle and density excitation frequencies, $\bar{\omega}_{SP}$ and $\bar{\omega}_0$, will lie close together.

1. Roton

In Fig. 8 we show $S(Q,\omega)$ for the roton Q at SVP at three temperatures compared with the observed intensity. As T decreases below T_λ, we again see the quasiparticle peak rapidly emerging in $S(Q,\omega)$. We see also a rapid loss of intensity immediately below the quasiparticle peak. This loss of intensity is particularly unusual because it takes place over a narrow temperature range of 0.4 K immediately below T_λ. It is difficult to explain this in terms of thermal factors. The loss of intensity is reproduced in the model because the zero in the numerator of $S(Q,\omega)$ at $\omega = \bar{\omega}_{SP}$ cancels out the intensity in the density component which peaks at $\bar{\omega}_0$ as soon as T drops below T_λ. At SVP, $\bar{\omega}_0 \approx \omega_{SP}$. In the model, there remains some intensity at low ω at $T = 1.79$ K not seen in the data. This could be removed in the model by allowing Γ_0 to decrease with decreasing T but we have kept Γ_0 constant for simplicity.

From Figs. 6 and 8 we see that, at the roton Q and low T, all of the intensity is confined to a single sharp peak arising from the quasiparticle. One of the challenges of this interpretation has been to show that, although the quasiparticle part of $S(Q,\omega)$ is weighted by $n_0(T)$ and $n_0(T)$ is small, all of the intensity can appear in the quasiparticle peak at low T for the roton. This challenge is clearly met in Figs. 6 and 8.

2. Beyond the roton

In Figs. 9 and 10 we show $S(Q,\omega)$ at $Q = 2.3$ and 2.5 Å^{-1} calculated at $T = 1.30$ K and $T = T_\lambda = 2.17$ K from (32) compared with the observed intensity at $T = 1.30$ K. In each case the quasiparticle peak ω_{SP} lies below the density excitation peak ω_0. The coupling $\Delta(T)$ appears to weaken with increasing Q. At $Q = 2.5$ Å^{-1}, a

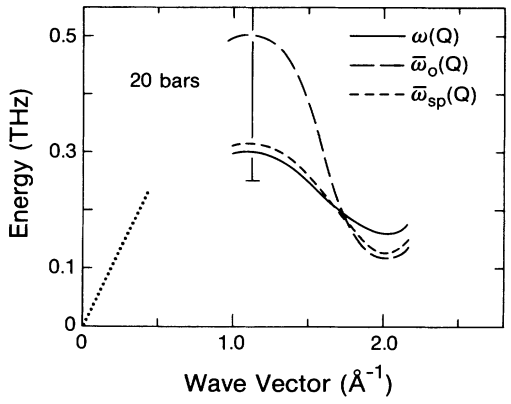

FIG. 7. Schematic diagram of the phonon-roton energy, $\omega(Q)$ [position of sharp peak of $S(Q,\omega)$ at low T] and of $\bar{\omega}_0$ and $\bar{\omega}_{SP}$, the uncoupled density and quasiparticle energies at $p = 20$ bars based on Table I. The dotted line is the sound velocity ($\omega/Q = 350$ m/sec at $Q \to 0$ estimated from data at $p = 24$ bars, Ref. 37).

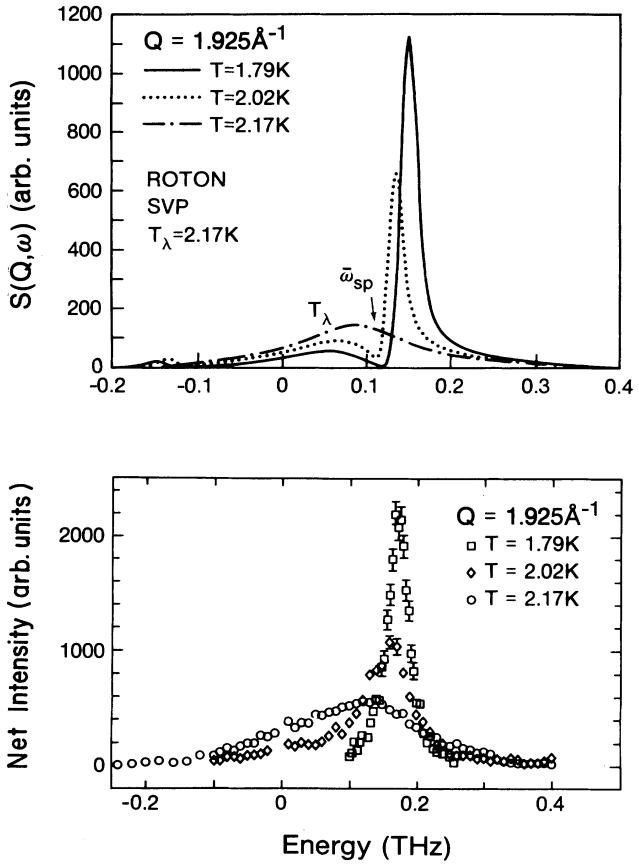

FIG. 8. Roton at $Q = 1.925$ Å^{-1} and SVP; as in Fig. 6 using parameters in Table II with Gaussian of FWHM of 0.0153 THz and data from Ref. 18.

very small coupling reproduces the weak quasiparticle peak in the observed intensity at $T=1.30$ K. Since $\Delta(T)$ is not large and $\bar{\omega}_{SP}$ and $\bar{\omega}_0$ are well separated, the density component of $S(Q,\omega)$ changes little with T. At these higher Q's, the chief effect of the coupling is to bring the quasiparticle peak into $S(Q,\omega)$ as T is lowered below T_λ, as suggested from (8). When the coupling is weak, (8) is a useful and representative expression. The observed width of the quasiparticle peak results from the resolution width.

In Fig. 11 we plot $\bar{\omega}_{SP}$, $\bar{\omega}_0$, and the quasiparticle peak position, $\omega(Q)$, at low T (the phonon-roton energy) at SVP. Again we see that $\bar{\omega}_{SP}(Q)$and $\omega(Q)$ cross at $Q\approx 1.5$ Å^{-1}.

3. *Quasiparticle lifetime*

In all the above $S(Q,\omega)$ we have set the quasiparticle half-width Γ_{SP} equal to zero. This is fundamentally for simplicity and to indicate in the model only that $\Gamma_{SP}\ll\Gamma_0$ at the maxon, roton, and higher-Q values. We do expect Γ_{SP} to increase with increasing T and $\Gamma_{SP}(T)$ has been extracted from experiment at several Q values.[24]

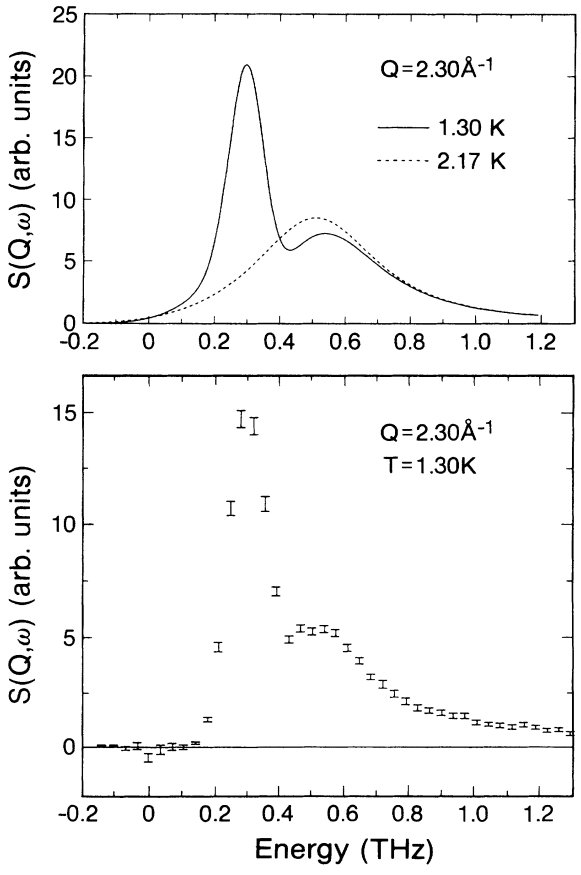

FIG. 9. $Q=2.30$ Å^{-1} and SVP; $S(Q,\omega)$ from (32) at $T=1.30$ K and $T_\lambda=2.17$ K using parameters from Table II and folded with a Gaussian of FWHM of 0.12 THz compared with data at $T=1.30$ K from Ref. 41.

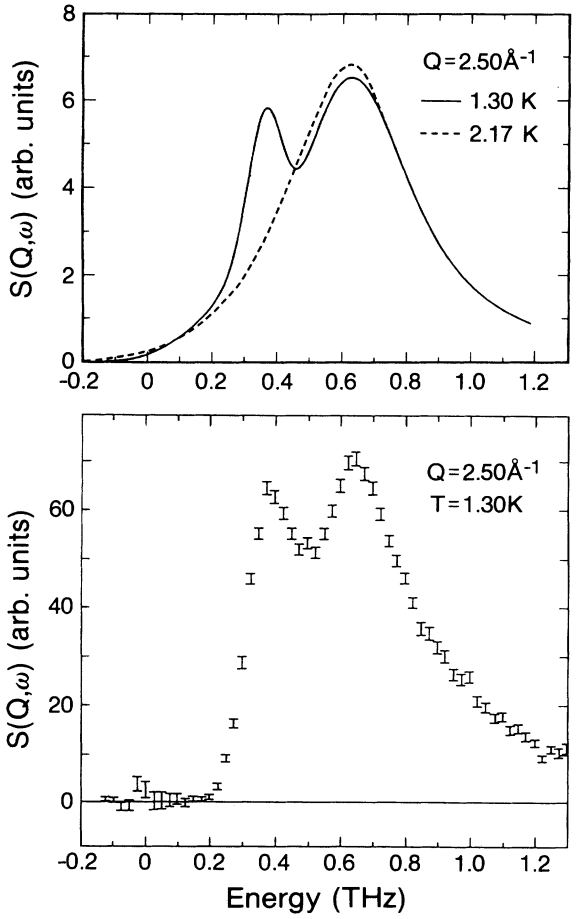

FIG. 10. As Fig. 9 for $Q=2.50$ Å^{-1}.

For example, at the roton at SVP, $\Gamma_{SP}(T)\simeq 0.001$ THz at $T=1.3$ K and $\Gamma_{SP}(T)\simeq 0.03$ THz at $T=2.0$ K. A precise $\Gamma_{SP}(T)$ is beyond the precision of the present crude model.

Only in the case of the maxon at $p=20$ bars does a finite Γ_{SP} clearly improve the agreement of $S(Q,\omega)$ with experiment at low T. In Fig. 12 we compare $S(Q,\omega)$ cal-

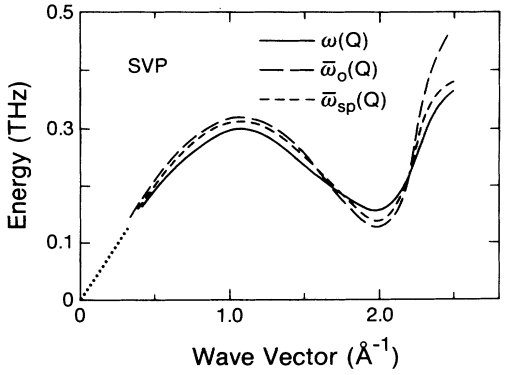

FIG. 11. As Fig. 7 at SVP using $\bar{\omega}_0$ and $\bar{\omega}_{SP}$ from Table II and sound velocity $\omega/Q=240$ m/sec at $Q\to 0$ from Ref. 38.

culate from the full result (31) for $\Gamma_{SP}=0$ and 0.01 THz. When Γ_{SP} is increased, the quasiparticle peak broadens and the dip in $S(Q,\omega)$ above the quasiparticle peak fills in. The relation between Γ_{SP} and filling in the dip is interesting. Γ_{SP} at the maxon and $T\simeq 1.3$ K, as obtained from observed values[22,25] of the peak width, does increase with pressure. From Fig. 4, the dip fills in as pressure is increased. It is interesting that these two effects are correlated here. This broadening may also explain why the structure in $S(Q,\omega)$ at high ω, seen in Fig. 4 at SVP, disappears at $p=25$ bars. A more complete model including multiexcitation contributions is needed to address this question.

IV. DISCUSSION

A. The interpretation

The present picture of excitations in superfluid ^{4}He has two components. When there is a condensate, quasiparticle excitations of the single-particle Green function G become a component of the total density response, χ, as shown in (8). The weight of G in χ depends on the condensate $n_0(T)$ through the vertex function $\Lambda=n_0^{1/2}[1+P(Q,\omega)]$. The second component of χ is χ', the density response of the atoms lying above the condensate. Thus, when $n_0(T)$ is finite, the quasiparticle excitations can be observed in $S(Q,\omega)$.

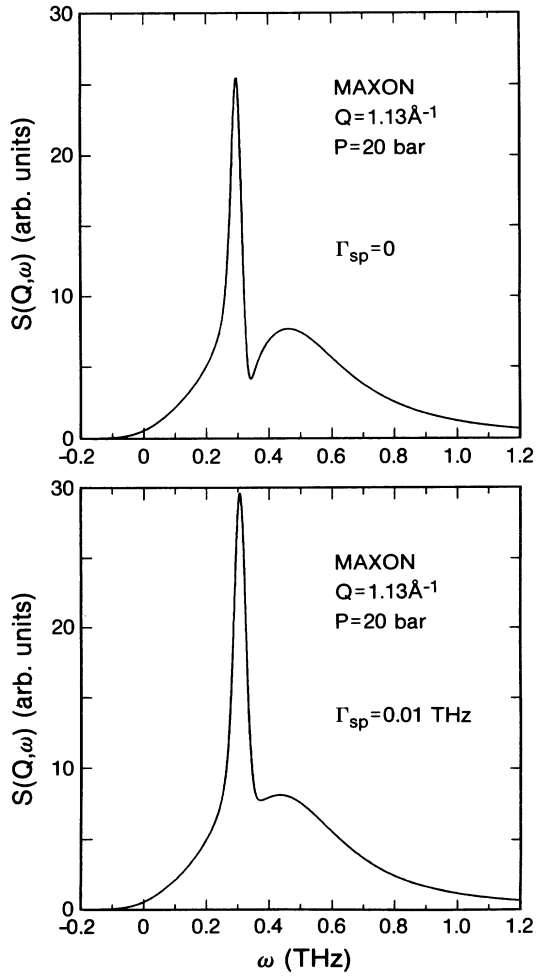

FIG. 12. Maxon at $Q=1.13$ Å^{-1} and $p=20$ bars: $S(Q,\omega)$ from (32) with parameters of Table I comparing $\Gamma_{SP}=0$ and $\Gamma_{SP}=0.01$ THz.

Equation (8) is a useful representation when $\chi'(Q,\omega)$ is a broad function of ω, the quasiparticle excitation is sharp and the coupling between the two via the condensate is weak. Under these circumstances, the quasiparticle excitation can be clearly observed in $S(Q,\omega)$ as a sharp component lying on broad scattering. This appears to be the case at $Q=2.5$ Å^{-1} as shown in Fig. 10. There the quasiparticle excitation appears as a sharp peak at lower ω below the broad density component of χ', which peaks near the free-atom recoil frequency $\omega_R=\hbar Q^2/2m$ ($\omega_R=0.79$ THz at $Q=2.5$ Å^{-1}). As T increases to T_λ, where $n_0(T)=0$, the sharp component disappears from $S(Q,\omega)$. It is the position of the sharp peak which is traditionally identified[9,24] as the phonon-roton energy at higher Q. The peak in G clearly leads to a peak in the density response and is therefore observable in $S(Q,\omega)$. However, the peak originates in G and can therefore be called a quasiparticle excitation. The intensity in this peak vanishes[9] at $Q\simeq 3.4$ Å^{-1}.

For $2.3\le Q\le 3.4$ Å^{-1}, there is a close analogy between $S(Q,\omega)$ in superfluid ^{4}He and in an anharmonic solid. In a solid, $\chi(Q,\omega)$ can be written in a form identical to (8) as[30]

$$\chi(Q,\omega)=R(Q,\omega)G_1R(Q,\omega)+\chi_M(Q,\omega)\ , \tag{37}$$

where G_1 is the one-phonon Green function, χ_M is the multiphonon response, and $R(Q,\omega)$ contains interference terms between the one and multiphonon components of χ. In a solid, $\chi_M(Q,\omega)$ is always a broad function of ω. The sharp structure in $\chi(Q,\omega)$ comes from the sharp one-phonon peak in $G_1(Q,\omega)$. We observe one-phonon energies in $\chi(Q,\omega)$ of (37) using neutrons in exactly the same way as we observe quasiparticle excitations of G in χ in superfluid ^{4}He. Both contribute to the density response. In a highly anharmonic solid, the interference terms[30] in $R(Q,\omega)$ can be large. This *may*[34] also be the case in superfluid ^{4}He.

Superfluid ^{4}He differs from an anharmonic solid in that χ', the density response of the atoms above the condensate, can also have sharp structure characteristic of a collective excitation. In this event the simple separation of χ into two additive terms in (8) is not useful. Indeed, at low Q in the phonon region, the density component is sharp characteristic of a collective mode—as indicated from sharp peak observed in normal ^{4}He where the $\Lambda G\Lambda$ term of (8) vanishes. We expect normal ^{4}He to support a collective density or phonon mode[21,32] at low Q as do other liquids.[35,36] As noted in Sec. II, the density and quasiparticle spectral functions share the same denominator when $n_0(T)\neq 0$. Thus, when the excitations in G and χ are sharp, the quasiparticle and density response of superfluid ^{4}He is identical and the two excitations cannot be distinguished. This will be the case in superfluid ^{4}He

at low Q. The chief thermal effect at low Q is a broadening of the sharp mode with increasing T.

As Q increases from the phonon to the maxon and roton regions, the density response of the atoms lying above the condensate broadens—as indicated from the scattering data in normal ^{4}He. In this Q region, the quasiparticle excitation remains sharp, as suggested by the data in superfluid ^{4}He at low T. At the same time, the coupling between the uncoupled density and quasiparticle excitations is strong. Because of this strong coupling, (8) is still not very useful and $S(Q,\omega)$ is complicated. It is primarily in this region of Q that we have attempted to model $S(Q,\omega)$ in a simple way based on the dielectric formulation Bose fluids. Specifically, we seek to display, in a simple way, how the existence of a sharp quasiparticle peak in $S(Q,\omega)$ depends on the condensate $n_0(T)$ and disappears from $S(Q,\omega)$ as T is increased into the normal phase. We now examine this simple model closely in order to study the parameters in it and reveal its limits.

B. The model

We begin in normal ^{4}He where $\chi(Q,\omega)$ is represented by (26),

$$\chi(Q,\omega)=\frac{\tilde{N}_R}{\omega^2-\bar{\omega}_0^2(Q)+2i\omega\Gamma_0(Q)} . \tag{38}$$

This may be derived as a phonon χ or from a random-phase-approximation-(RPA-) like method. In the application of (38), we fitted the corresponding $S(Q,\omega)$ to the single density excitation at low Q and focused on reproducing the low-frequency region of the data at higher Q. The observed intensity at higher Q, especially at the roton in normal ^{4}He (see Fig. 6), has high-frequency tails. Since the present $S(Q,\omega)$ is fitted to the lower-ω region of the intensity and it does not reproduce the high-frequency tails, χ in (38) and $S(Q,\omega)$ in (27) will not reproduce sum rules. Crudely, (38) is approximately the single excitation component of $\chi(Q,\omega)$ for Q's up to the roton Q and does not include the whole of $S(Q,\omega)$.

A direct fit of (27) to the data of Andersen *et al.*[37] yields the values of $\bar{\omega}_0(Q)$ and $\Gamma_0(Q)$ for normal ^{4}He shown in the upper half of Fig. 13. These are empirical values of $\bar{\omega}_0(Q)$ and $\Gamma_0(Q)$. In Fig. 13 the height of the bars is $2\Gamma_0(Q)$ and the bar is centered at $\omega_Q=(\bar{\omega}_0^2-\Gamma_0^2)^{1/2}$, the energy that has traditionally been used to identify the phonon-roton energy. That is, the "harmonic-oscillator" function (27) may be reexpressed as a sum of two "Lorentzian" functions,[25]

$$\frac{(2\omega\Gamma_0)}{(\omega^2-\bar{\omega}_0^2)^2+(2\omega\Gamma_0)^2} = \frac{1}{2\omega_Q}\left[\frac{\Gamma_0}{(\omega-\omega_Q)^2+\Gamma_Q^2}-\frac{\Gamma_Q}{(\omega+\omega_Q)^2+\Gamma_Q^2}\right] , \tag{39}$$

where $\bar{\omega}_0^2=\omega_Q^2+\Gamma_0^2$. The rhs of (39) has traditionally[9,24] been fitted to data with ω_Q defined as the phonon-roton energy. $\bar{\omega}_0$ is strictly the more fundamental parameter.

In normal ^{4}He at low Q, where $\Gamma_0<\bar{\omega}_0$ in Fig. 13, $\bar{\omega}_0(Q)$ and $\Gamma_0(Q)$ may be immediately interpreted as the energy and half-width [lifetime $\tau(Q)=\Gamma_0^{-1}(Q)$] of the collective density excitation. The model does not attempt to develop or derive the collective mode from single-particle excitations; it rather assumes its existence. In the maxon and roton regions where Γ_0 is large ($\Gamma_0\simeq\bar{\omega}_0$), it is difficult to say whether a well-defined collective excitation exists. At the maxon and roton Q, where $\Gamma_0\simeq\bar{\omega}_0$, $\bar{\omega}_0$ and Γ_0 are better interpreted as an energy and width characterizing weakly interacting particle-hole excitations.

In modeling the dielectric formulation for higher Q in superfluid ^{4}He, we represented the uncoupled density response of the atoms above the condensate by

$$\tilde{\chi}_R=\frac{\chi}{1+v(Q)\chi}=\frac{\tilde{N}_R}{\omega^2-(\bar{\omega}_0^2-\alpha)+i2\omega\Gamma_0} , \tag{40}$$

where $\alpha=v(Q)\tilde{N}_R$ and $\Omega^2=\bar{\omega}_0^2-\alpha$. $\tilde{\chi}_R$ is intended to represent approximately a Lindhard function for the atoms above the condensate having renormalized energies, i.e,

$$\begin{aligned}\chi_L&=\frac{1}{V}\sum_k\frac{n_k-n_{k+Q}}{\omega-(\varepsilon_{k+Q}-\varepsilon_k)+i\eta}\\&=\frac{1}{V}\sum_k\frac{2\omega_k n_k}{\omega^2-\omega_{kq}^2+i2\omega\eta}\\&\simeq\frac{N_R}{\omega^2-\Omega^2+i2\omega\Gamma_0} .\end{aligned} \tag{41}$$

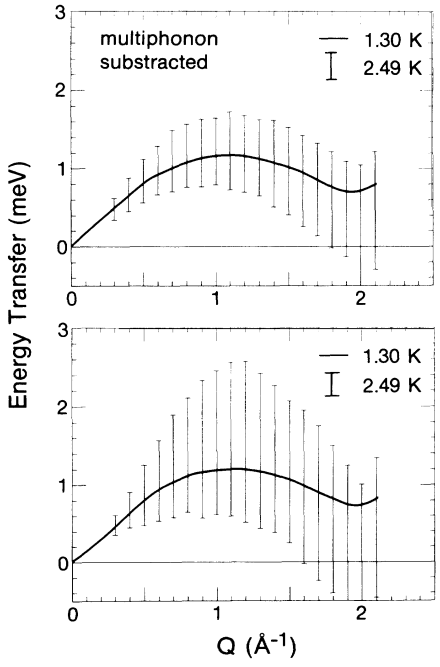

FIG. 13. The bars show the width ($2\Gamma_0$) of the scattering intensity at $T=2.49$ K in normal ^{4}He obtained by the least-squares fit of (27) to the data of Andersen *et al.* (Ref. 37). The bars are centered at $\omega_Q=(\bar{\omega}_0^2-\Gamma_0^2)^{1/2}$. The solid line is the position of the sharp peak at $T=1.30$ K (the phonon-roton curve). At $T=1.30$ K, the intrinsic width is within the solid line.

TABLE II. As in Table I for saturated vapor pressure (SVP).

Q (Å^{-1})	$\bar{\omega}_0$	Γ_0	$\bar{\omega}_{SP}$	Γ_{SP}	Δ	$\alpha/\bar{\omega}_0^2$	$\omega(Q)$
1.1 (maxon)	0.32	0.12	0.32	0	−0.015	−0.5	0.29
1.925 (roton)	0.119	0.075	0.12	0	0.0155	0.5	0.18
2.30	0.55	0.21	0.33	0	−0.012	−0.3	0.30
2.50	0.66	0.22	0.38	0	−0.004	−0.4	0.37

Ω^2 corresponds to an average of the difference in uncoupled quasiparticle energies, i.e., $\Omega^2=\langle\omega_{kq}^2\rangle=\langle(\varepsilon_{k+q}-\varepsilon_k)^2\rangle$. Γ_0 represents the difference in lifetime of these energies. In a consistent theory, ε_k should lie close to the uncoupled quasiparticle energies $\bar{\omega}_{SP}$.

We have identified $\bar{\omega}_{SP}$ with the position of the observed dip in $S(Q,\omega)$ in superfluid ^{4}He, as shown in Fig. 4. Using the data of Andersen *et al.*,[39] this yields the $\bar{\omega}_{SP}$ in superfluid ^{4}He shown in Fig. 11 which follow a phonon-roton-like curve. The parameter α in (40) and $\Delta(T)$ are determined to get the sharp peak position and height correct at $T=1.3$ K. Using α from Tables I and II, we see $\Omega^2=\bar{\omega}_0^2-\alpha=\bar{\omega}_0^2(1-\alpha/\bar{\omega}_0^2)$ lies above $\bar{\omega}_0$ at the maxon and below $\bar{\omega}_0$ at the roton. $v(Q)$ is the weak, renormalized interaction which shifts Ω^2 to $\bar{\omega}_0^2=\Omega^2+v(Q)\tilde{N}_R$ in χ. We emphasize that $\bar{\omega}_{SP}$ and α have been determined in superfluid ^{4}He. We do expect $\bar{\omega}_{SP}$ to differ in normal and superfluid ^{4}He. Especially, the development of a collective excitation will be different. As noted, a collective excitation is assumed and not developed here.

C. *f*-sum rule

The contribution of a model $\chi(Q,\omega)$ to the f-sum rule, $M=\int d\omega\,\omega S(Q,\omega)=\hbar Q^2/2m$, may be obtained as

$$M_c=\frac{\omega^2}{2}\lim_{\omega\to\infty}\chi(Q,\omega)\ . \tag{42}$$

In the present model, we have focused on fitting the low-ω region of $S(Q,\omega)$. In the cases in which most of the intensity is at low ω or there is no high-energy tail, we expect $M_c\simeq M=\hbar Q^2/2m$. For example, we expect $M_c\simeq M$ at $Q=2.5$ Å^{-1}, where $S(Q,\omega)$ in (27) apparently reproduces all of the observed intensity quite well.

In normal ^{4}He, using (38) we have,

$$M_c^*=\frac{\tilde{N}_R}{2}=\frac{\alpha}{2v(Q)}\ , \tag{43}$$

where the star denotes normal ^{4}He. If $v(Q)$ were known, the contribution to M_c^* could be evaluated. At $Q=2.5$ Å^{-1}, where we expect $M_c^*\simeq M$, we may use (43) to determine $\tilde{N}_R$ and $v(Q)$ giving $\tilde{N}_R=\hbar Q^2/m$ and $v(Q)=5.4$ K, respectively. Thus, $v(Q)$ is small as expected and quite different from the potential needed to develop a collective excitation. At low Q, where $\bar{\omega}_0^2=c_0Q^2$ and where we find $\alpha/\bar{\omega}_0^2$ is approximately constant, $v(Q)=\alpha/2M_c^*\simeq\alpha/2\omega_R$ is approximately independent of Q. In superfluid ^{4}He, using (19) and (17) for χ, we have

$$M_c=\frac{1}{2v(Q)}(\alpha+\Delta)=\frac{\alpha}{2v(Q)}\left[1+\frac{\Delta}{\alpha}\right] \tag{44}$$

and

$$\frac{M_c}{M_c^*}=1+\frac{\Delta}{\alpha}\ . \tag{45}$$

Clearly, if $M_c=M_c^*=M$, we expect $M_c/M_c^*=1$. At the maxon, the roton, and $Q=2.5$ Å^{-1}, we obtain $M_c/M_c^*=1.3$, 3.6, and 1.02 using Δ/α at SVP from Table II. At $Q=2.5$ Å^{-1}, $M_c/M_c^*=1.02$ because χ in (38) describes the whole of $S(Q,\omega)$ well so that $M_c^*\simeq M$. In this case we expect $M_c/M_c^*\simeq1$. At the roton M_c^* misses the very large contribution to M from the high-frequency tail. This tail is much smaller at lower temperature in superfluid ^{4}He (see Fig. 6). Thus, we expect M_c/M_c^* to be large at the roton where the quasiparticle peak at low ω is large in superfluid ^{4}He. A similar effect but less pronounced occurs at the maxon. Without a description of the high-frequency tail, we cannot make further use of the f-sum rule.

At low Q, we may estimate $S(Q)$ using (27) and (38) which gives

$$S(Q)=\frac{\tilde{N}_R}{2\bar{\omega}_0}[2n(\bar{\omega}_0)+1]\ . \tag{46}$$

For $Q\gtrsim0.2$ Å^{-1}, but low Q, $n(\bar{\omega}_0)$ is negligible and $S(Q)=\tilde{N}_R/2\bar{\omega}_0=\hbar Q/2Mc_0$, which follows using the f-sum-rule result for $\tilde{N}_R$.

The present model is intended to be illustrative and it is possible to overinterpret the parameters and lose the broad meaning. Other parametrizations are clearly possible.

D. Thermodynamic properties.

The characteristic excitations of liquid ^{4}He have, since Landau,[1] been used to evaluate the thermodynamic properties of superfluid ^{4}He. The low-lying excitations in the phonon and roton regions are predominant at low T. The thermodynamic properties are evaluated[40] assuming there is a single excitation at each wave vector Q.

In the present model, we have included density and quasiparticle excitations. An important result of the dielectric formulation is that the density (χ) and quasiparticle (G) propagators share the same denominator as seen from (20) and (22). If the excitations have small widths, we therefore expect χ and G to have common poles. In this sense there is only a single excitation in the fluid. This point was emphasized by Gavoret and

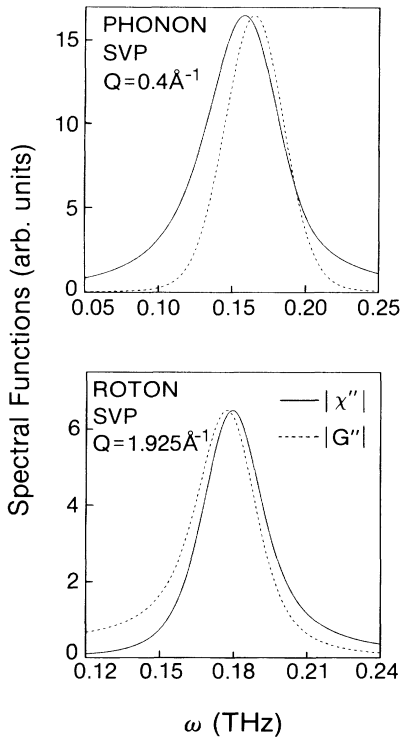

FIG. 14. Density and quasiparticle spectral functions in superfluid ^{4}He from (31) and (35) with the parameters in Table II and $\Gamma_{SP}=0.0017$ THz at $T=1.30$ K.

Nozières[12] who showed that the excitations of χ and G have the same linear dependence on Q, $\omega(Q)=c_0Q$ at low Q.

To emphasize this point we have evaluated the spectral functions of χ and G from (31) and (35) in the phonon and roton regions at SVP, using the parameters listed in Table II for the roton, setting $\bar{\omega}_{SP}$ close to $\bar{\omega}_0$ for the phonon, and $\Gamma_{SP}=0.0017$ THz for both the roton and the phonon. The results are shown in Fig. 14 and we see that both χ'' and G'' are confined to a single sharp peak at low T. χ'' and G'' are slightly displaced from one another due to the different numerators in (31) and (35). This shows that the density and quasiparticle excitation energies track each other closely when the excitations are sharp in the present model.

In summary, the goal here has been to illustrate how the temperature dependence of $S(Q,\omega)$ can be reproduced in a simple model based on the dielectric formulation. Specifically, we wish to reproduce the shaper peak in $S(Q,\omega)$ at the maxon, roton, and higher Q as a quasiparticle peak and illustrate how this peak disappears from $S(Q,\omega)$ following $n_0(T)$. We see that this structure can be obtained keeping all parameters constant except $n_0(T)$. The temperature dependence might be improved by using $n_0(T)$ for liquid ^{4}He rather than the Bose-gas $n_0(T)$ used here. The model is extremely simple, has clear limitations, and is only a first step toward describing $S(Q,\omega)$ using the dielectric formulation. Particularly, a clearer basis in microscopic theory and addition of higher ω components of $S(Q,\omega)$ is needed.

ACKNOWLEDGMENTS

It is a pleasure to acknowledge Allan Griffin, with whom many ideas and an initial form of the present model have been developed (Ref. 20). It is also a pleasure to thank William Stirling and Bjorn Fåk for valuable discussions and for permission to use unpublished data in Fig. 13 and Figs. 9 and 10, respectively. Dr. Piotr Findeisen provided key numerical assistance and Ken Andersen prepared Fig. 13. The financial support from NSERC, Canada and NATO is gratefully acknowledged.

*Present address: Department of Physics and Astronomy, University of Delaware, Newark, DE 19711.

[1]L. D. Landau, J. Phys. (Moscow) **5**, 71 (1941).
[2]L. D. Landau, J. Phys. (Moscow) **11**, 91 (1947).
[3]N.N. Bogoliubov, J. Phys. (Moscow) **11**, 23 (1947).
[4]R. P. Feynman, Phys. Rev. **94**, 262 (1954).
[5]R. P. Feynman and M. Cohen, Phys. Rev. **102**, 1189 (1956).
[6]C. E. Campbell, in *Progress in Liquid Physics,* edited by C. A. Croxton (Wiley, New York, 1978), p. 213; G. V. Chester, in *The Helium Liquids,* edited by J. G. M. Armitage and I. E. Farquhar (Academic, London, 1975), pp. 33 and 150.
[7]E. Manousakis and V. R. Pandharipande, Phys. Rev. B **33**, 150 (1986).
[8]A. Miller, D. Pines, and P. Nozières, Phys. Rev. **127**, 1452 (1962).
[9]A. D. B. Woods and R. A. Cowley, Rep. Prog. Phys. **36**, 1135 (1973).
[10]S. T. Beliaev, Zh. Eksp. Teor. Fiz. **34**, 417 (1958) [Sov. Phys. JETP **7**, 289 (1958)].
[11]N. Hugenholtz and D. Pines, Phys. Rev. **116**, 489 (1959).
[12]J. Gavoret and P. Nozières, Ann. Phys. (NY) **28**, 349 (1964).
[13]P. C. Hohenberg and P. C. Martin, Ann. Phys. (NY) **34**, 291 (1965).
[14]S.-k. Ma and C. W. Woo, Phys. Rev. **159**, 165 (1967).
[15]S.-k. Ma, H. Gould, and V. K. Wong, Phys. Rev. A **3**, 1453 (1971).
[16]A. Griffin and T. H. Cheung, Phys. Rev. A **7**, 2086 (1973).
[17]P. Szépfalusy and I. Kondor, Ann. Phys. (NY) **82**, 1 (1974).
[18]W. G. Stirling and H. R. Glyde, Phys. Rev. B **41**, 4224 (1990).
[19]H. R. Glyde and W. G. Stirling, in *PHONONS 89,* edited by S. Hunklinger, W. Ludwig, and G. Weiss (World Scientific, Hong Kong, 1990).
[20]H. R. Glyde and A. Griffin, Phys. Rev. Lett. **65**, 1454 (1990).
[21]D. Pines, in *Quantum Fluids,* edited by D. F. Brewer (North-Holland, Amsterdam, 1966), p. 257.
[22]A. D. B. Woods and E. C. Svensson, Phys. Rev. Lett. **41**, 974 (1978).
[23]A. Griffin, Can. J. Phys. **65**, 1368 (1987).
[24]H. R. Glyde and E. C. Svensson in *Methods of Experimental Physics,* edited by D. L. Price and K. Sköld (Academic, New

York, 1987), Vol. 23, Pt. B, p. 303.
[25]E. F. Talbot, H. R. Glyde, W. G. Stirling, and E. C. Svensson, Phys. Rev. B **38**, 11 229 (1988).
[26]A. D. B. Woods, Phys. Rev. Lett. **14**, 355 (1965).
[27]D. Pines, Physics Today **42**(2), 61 (1989).
[28]G. D. Mahan, *Many Particle Physics* (Plenum, New York, 1981).
[29]S. W. Lovesey, *Neutron Scattering,* 3rd ed. (Oxford University Press, Oxford, 1987), Vols. I and II.
[30]V. Ambegaokar, J. Conway, and G. Baym, in *Lattice Dynamics,* edited by R. F. Wallis (Pergamon, New York, 1965), p. 261; R. A. Cowley and W. J. L. Buyers, J. Phys. C **2**, 2262 (1969); H. Horner, Phys. Rev. Lett. **29**, 556 (1972); H. R. Glyde, Can. J. Phys. **52**, 2281 (1974).
[31]W. G. Stirling, in *Proceedings of the 2nd International Conference on Phonon Physics,* edited by J. Kollar, N. Kroó, N. Menyhard, and T. Siklos (World Scientific, Singapore, 1985), p. 829.
[32]C. H. Aldrich, III and D. Pines, J. Low Temp. Phys. **25**, 677 (1976), D. Pines, in *Highlights of Condensed Matter Theory,* edited by F. Bassani, F. Fumi, and M. P. Tosi (North-Holland, New York, 1985), p. 580.
[33]B. Dorner, J. D. Axe, and G. Shirane, Phys. Rev. B **6**, 1950 (1977).
[34]E. C. Svensson, P. Martel, V. F. Sears, and A. D. B. Woods, Can. J. Phys. **54**, 2178 (1976); H. R. Glyde, in *Condensed Matter Research Using Neutrons,* edited by S. W. Lovesey and R. Scherm (Plenum, New York, 1984), p. 95.
[35]H. G. Bell, A. Kollmar, B. Allfeld, and T. Springer, Phys. Lett. **45A**, 479 (1973); W. J. L. Buyers, V. F. Sears, P. A. Lonngi, and D. A. Lonngi, Phys. Rev. B **11**, 697 (1975).
[36]J. R. D. Copley and J. M. Rowe, Phys. Rev. Lett. **32**, 49 (1974); A. Rahman, *ibid.* **32**, 52 (1974); G. Jacucci, in *Condensed Matter Research Using Neutrons,* edited by S. W. Lovesey and R. Scherm (Plenum, New York, 1984).
[37]E. C. Svensson, A. D. B. Woods, and P. Martel, Phys. Rev. Lett. **29**, 1148 (1972).
[38]W. G. Stirling, in *75th Jubilee Conference on Helium-4,* edited by J. G. M. Armitage (World Scientifc, Singapore, 1983), p. 109.
[39]L. K. Andersen *et al.* (unpublished).
[40]R. J. Donnelly, J. A. Donnelly, and R. N. Hills, J. Low Temp. Phys. **44**, 471 (1981).
[41]B. Fåk and L. K. Andersen, Phys. Lett. (to be published).